COMPARATIVE ANALYSIS OF CFD AND ADAPTIVE NEURAL FUZZY INFERENCE SYSTEM FOR PREDICTING HEAT TRANSFER ENHANCEMENT IN WATER-FE_2O_3 NANOFLUIDS ACROSS VARIOUS FLOW REGIONS

[1*]Cristian Germán-Santiana Espín, [2]Byron Fernando-Castillo Parra, [3]Diana Katherine-Campoverde Santos, [4]Luis Buenaño

[1*,2,3]Professor, Facultad de Ciencias Pecuarias, Escuela Superior Politécnica de Chimborazo (ESPOCH), Panamericana Sur km 1 1/2, Riobamba, 060155, Ecuador.

[4]Professor, Facultad de Mecánica, Escuela Superior Politécnica de Chimborazo (ESPOCH), Panamericana Sur km 1 1/2, Riobamba, 060155, Ecuador.

Email : [1]santiana@espoch.edu.ec, [2]byron.castillo@espoch.edu.ec, [3]diana.campoverde@espoch.edu.ec, [4]lfbuenanio@espoch.edu.ec

Abstract

Models for enhancement of heat transfer in nanofluids made wide use of ANFIS and the multiphase Mixture model in recent years. These models originate from two separate but complementary branches of engineering: computational mechanics and machine intelligence. Not only have prior studies used only a small subset of nanofluid and flow parameters in their analyses, but no one has ever compared the two methods to determine which one is more applicable to certain flow regimes to forecast how much heat transfer development nanofluids will exhibit. The purpose of this study was to compare the accuracy of two methods—CFD and ANFIS in predicting the heat transfer improvement of water-Fe2O3 nanofluid for variety of nanofluid formations and flow characteristics, and recommend the method that would be most useful in predicting this enhancement for each flow regime. While ANFIS consistently outperforms the Mixture models in prediction of nanofluid heat transfer enhancement, the latter can sometimes produce results that differ greatly from experimental correlation; however, for nanofluid configurations, the Mixture model's predictions can be dependable (with 1% error).

Keywords*: Nanofluids, Mixture models, ANFIS, Fe2O3, Fuzzy System*

1. Introduction

Since the material was introduced by Choi and Eastman [1], researchers have performed a plethora of numerical studies and experimentation on heat transmission utilising nanofluids. The ease with which numerical simulation can anticipate the heat-transferring behaviour of nanofluids has made it a hot topic. Due to the method's popularity among specialists, several models have been developed in the past 20 years to simulate nanofluids using CFD. There are two main types of models utilised in these simulations: single-phase models and multiphase models [2]. A lot of recent studies have used both models, drawing parallels between the simulated and experimental data and correlations to draw conclusions. Although some research found more convincing results from single-phase models,

multiphase models generally better matched experimental data when it came to predicting the behaviour of nanofluids heat transfer. The optimal model was selected by comparing outputs of multi and single-phase models; the criterion for success is the model that produced the smallest discrepancy between the predicted and observed outcomes [3].

To study the convective heat transfer of H_2O / copper nanofluid with 0.3% particle concentration, authors [4] used single and multi-models. Results showed for two-phase model, there was an 8 % relative inaccuracy and for the one-phase model, it was 16 %. In their study of several PCs, Authors [5] used both single and multiphase techniques. They discovered that whereas the multiphase model could explain as much as single-phase model and 10% experimental data, could only explain an average variation of 1%. Alternatively, the single-phase model demonstrated a 7% variance in wall heat transfer predictions. According to authors [6], who examined 5 distinct nanoparticle concentrations, the average errors produced by the single phase model range of Re of water-magnesium oxide nanofluid flow were 11% and by 2% multiphase model. Compared to single-phase models, two-phase models offered more realistic predictions for laminar mixed convection flows with PCs below 2% [7]. Nanofluids comprising Cu, CuO, and Fe_2O_3 were studied by authors [8] in laminar flow via square-section conduit at PC levels up to 4% using a dispersion model to forecast Nu. For 0, 0.5 and 1% particle volume fractions for SiO2-water nanofluid, the Nusselt number could be 7.8% accurately predicted using the single phase flow in sinusoidal channels also 7.3% in trapezoidal channels. Evidence from studies conducted by researchers suggests that the Nusselt number may be predicted on circular tube with constant heat flux using either a discrete phase model (DPM) or a single-phase model. When comparing two models' predictions for the mean coefficient of heat transfer, an 11% discrepancy was noted. There was a 10% difference between the experimental and simulated Nusselt values, and the PC in this study ranged from 1% to 4%.

For their work on the heat transmission of a H_2O/Fe_2O_3 nanofluid, researchers [9] used a micro channel heat sink. According to their findings, single phase model was 31% and 36% off for 1 % and 2 % combinations of nanofluid, whereas two phase mixture model was 11.39% and 2% off for the same configurations. Using computational fluid dynamics (CFD) methods, authors [10] analysed turbulent heat transfer of a hybrid nanofluid (Fe_2O_3-CuO/water). A discrepancy of 8.1%, 10.2%, and 12.5% was discovered by the researchers between the experimental and simulation outcomes for DPM model, Mixture model, and Eulerian model respectively. Researchers discovered a discrepancy of about 40% among experimental data and single phase CFD simulation when they examined nanofluid heat transfer of a copper oxide/H_2O in horizontal coil.

In the application of dual phase mixture model to water-Fe_2O_3 nanofluid, authors [11] utilised three distinct PCs. While looking at heat transfer improvements, this study found that maximum discrepancy among simulation and experimental outcome is 8%. Using the same methodology, researchers [12] compared the simulated and experimental results using a single, Eulerian model, and multiphase Mixture model, finding that variations are less than 9%, 14%, and 18%. Researchers [13] investigated a multiphase mixture using a VOF model with same nanofluid, boundary conditions, and geometry. Four distinct Re and three distinct PCs were considered by the researchers. The two models performed admirably. Errors reached approximately 30% at 1% and 6% PC, whereas the difference from experimental correlation data at 4% PC was 12%. The results showed that for 1% PC, both models under-estimated the heat transfer improvement, whereas for 4% and 6% PC, they overestimated it.

The multiphase Mixture model is among popular multiphase models used to predict the improvement of nanofluids heat transfer within field of computational mechanics. Also hailing from the AI realm is ANFIS. Researchers have found both approaches to be quite trustworthy for making case-to-case predictions of nanofluid heat transfer enhancement; nevertheless, there are certain gaps in the study on how to model nanofluid heat transfer using these two methods. The first issue is that all the prior work on ANFIS heat transfer enhancement modelling of nanofluids has relied on a small subset of possible nanofluid geometries and turbulence levels. Similar to how the majority of CFD research

employing the Mixture model perform. It is necessary to compare these two methods for predicting the improvement of heat transfer on nanofluids for particular flow regions, but no study has done so yet. This is problematic for a number of reasons, including the fact that both methods are labor-intensive and have their own set of advantages and disadvantages. This research made use of the CFD in addition to ANFIS model. The objective is to compare the two methods' efficiencies with experimental correlation data in order to determine which one is better at forecasting the heat transfer improvement of water-iron oxide nanofluids over various applications of Re concentrations and nanoparticle to identify which method is better at determining heat transfer improvement for every flow region.

2. CFD modeling

For the incompressible flow and steady-state conditions, multiphase Mixture model was used in the computational fluid dynamics (CFD) modelling of a 2-dimensional geometry, with the realisable k-ε turbulence model being considered.

2.1. Geometry

In this study, a circular pipe of Φ10 mm, 1 m in length, and positioned horizontal w.r.t. ground is considered.

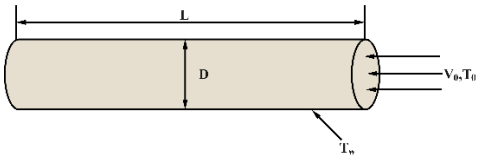

Figure 1. Circular pipe

2.1. Turbulence modeling

The turbulent flow of nanofluid has been modelled using realisable turbulence model k-ε. This model takes consider both turbulent kinetic energy (k) and its dissipation rate (ε). According to this research, they are best understood as [14]:

$\partial\partial t\ (\rho mk) + \partial\partial x\ (\rho mkv\rightarrow m) = \partial\partial x\ [(\mu t,m+\mu t,m\sigma k)\ \partial k\partial x] + Gk,m + Gb - \rho m\varepsilon - YM + Sk$

$\partial\partial t\ (\rho m\varepsilon) + \partial\partial x\ (\rho m\varepsilon v\rightarrow m) = \partial\partial x\ [(\mu t,m+\mu t,m\sigma\varepsilon)\ \partial\varepsilon\partial x] + \rho mC1S\varepsilon - \rho mC2\varepsilon 2k+v\varepsilon + C1\varepsilon\ \varepsilon kC3\varepsilon Gb+S\varepsilon$ (1)

$$C1=\max\ [0.43,\eta\eta+5] \quad (2)$$

$$\eta=2SijSij\ k\varepsilon \quad (3)$$

Eddy viscosity (μt,m), formation of turbulent kinetic energy (Gk,m) as result of mean velocity gradients, buoyance's contribution to turbulent kinetic energy (Gb), and the fluctuating dilation in compressible turbulence (YM) as a whole are represented in the equations described above. The values of C2 and C1ε stand as constants. The Turing Transform for k and ε is denoted by σk and σε, respectively. The following is a definition of the model constants:

$$C_{1\varepsilon} = 1.44,\ C_2 = 1.9,\ \text{and}\ \sigma k=1\ \text{and}\ \sigma\varepsilon=1.2$$

2.2. Thermophysical properties and boundary conditions

Utilizing the subsequent mathematical formulas, the essential thermophysical characteristics of nanofluids, including density (ρnf), specific heat (Cpnf), viscocity (μnf), and thermal conductivity (λnf), have been computed [15]:

$$\rho nf=(1-\varphi)\rho bf+\varphi\rho p \quad (4)$$

$$C_{pnf}=(1-\varphi)C_{pbf}+\varphi C_{pp} \quad (5)$$

$$\mu_r=\mu_{nf}\mu_{bf}=123\ \varphi^2+7.3\varphi+1 \quad (6)$$

$$\lambda_r=\lambda_{nf}\lambda_{bf}=4.97\ \varphi^2+2.72\ \varphi+1 \quad (7)$$

The relative thermal conductivity (λ_r) and relative viscosity (μ_r) of nanofluid is denoted as λ_r and λ_r, respectively.

Three areas of the pipe were considered when determining the boundary conditions: the entrance, the walls, and the outflow. A condition of uniform velocity was enforced at the inflow. The intake velocity (Vo) was determined as Reynolds number was raised from 10,000 - 90,000. A constant temperature (T0) of 293 K was maintained for the nanofluid at the input. A condition of constant wall temperature was adjusted at the pipe walls. At 350 K, the wall temperature (Tw) remained unchanged. The flow along the walls was not subject to a slide condition. The gauge pressure (Pout) was maintained constant at 0 Pa at exit of pipe due to a pressure condition. Following is an equational representation of boundary conditions:

$$T_w=350K \quad (8)$$

$$T_0=293K \quad (9)$$

$$P_{out}=0\ Pa \quad (10)$$

$$\left.\frac{dx}{dt}\right|_{wall}=0\ m/s \quad (11)$$

$$V_o=\left.\frac{dx}{dt}\right|_{inlet}=Re*\mu_{nf}\rho_{nf}*D \quad (12)$$

2.3. Mesh independence test

In order to run the simulation, ANSYS 2021 R1's 2-dimensional geometry was used to construct an orthogonal structured mesh. This mesh was then divided with horizontal and vertical edges using two different edge sizing. In order to perform the mesh independence test, divisions with vertical edges are adjusted from 20 to 130. To capture boundary layers, mesh was made denser at the walls using the biassing method. The mesh independence study was conducted by changing the number of divisions at intake and using mean outlet temperature as output parameter (Figure 2).

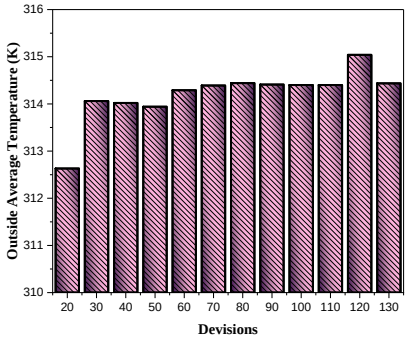

Figure 2. study of Mesh Independence

After considering the maximum outlet parameter deviations in prior mesh and fact that computing time is increased by a high-density mesh, it was concluded that an optimal mesh would have 50 divisions at the inlet, 37,771 nodes, and 37,000 elements. We checked the skewness and mesh quality to find the best mesh. The mesh had an average skewness of 1.3062×10^{-10} and a maximum skewness of 1.3368×10^{-10}, all of which are within the allowed range. The aspect ratio is 3.96494. The optimal orthogonal meshing is shown by orthogonal quality of mesh, which is equal to one.

2.4. Approach to numerical solutions

For the simulations, CFD solver FLUENT 2021 was utilised. Using a segregated solver, governing equations are resolved utilizing finite volume approach. The volume fraction are discretized utilizing the QUICK arrangement, while convection terms, energy, turbulent kinetic energy, and turbulent kinetic energy dissipation rate were discretized using the second-order upwind strategy. Figure 3 shows the utilized Pressure Implicit with Splitting of Operators (PISO) technique for velocity-pressure coupling handling. Because it is an improvement on the Semi-Implicit Method for Pressure Linked Equations (SIMPLE) technique, this one uses much less processing power. Factors including energy, mass, velocity components, volume fraction, turbulent kinetic energy, and turbulent kinetic energy dissipation rate formed on basis of the convergence criterion. A residual value of 10^{-6} was utilised in the energy equation, whilst residual values of 10^{-4} were employed in the continuity, velocity, turbulent kinetic energy, and turbulent kinetic energy dissipation rate equations.

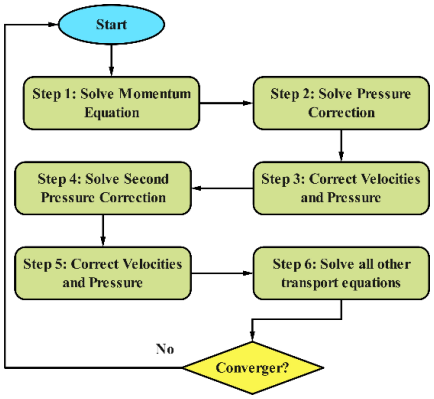

Figure 3. Algorithm of segregated PISO

2.5. Validation

Based on experimental correlation, finding from authors [16], this investigation verified the Mixture model parameters. A nanofluid including water and iron oxide was validated. The simulation results were obtained using the identical boundary conditions that were described before in this paper. The Re was varied between 10,000 and 90,000 for 2.6 % PC in order to validate the process. Verification was carried out by comparing the Nu to Re. Equations for calculating the Reynolds number and the Nusselt number are as follows:

$$Re=\rho VD\mu \quad (13)$$

$$Nu=hD\lambda nf \quad (14)$$

This is where the variables V, h, and D stand for the developed region flow velocity, pipe diameter, and convective heat transfer coefficient, respectively. The λnf represents the nanofluid's thermal conductivity. Using a PC of 2.5 % and an experimental correlation error of 6 to 10 %, Fig 4 shows comparison of simulated and experimental Nu vs. Re for the Mixture model. For nine distinct Reynolds numbers, the Mixture model has an average inaccuracy of 7.52%.

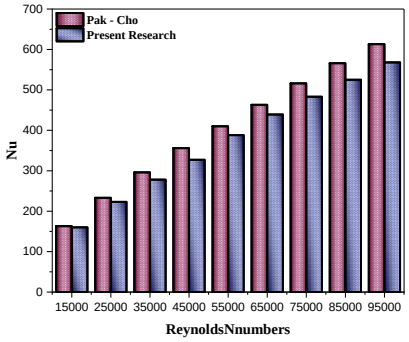

Figure 4. The 3% particle concentration on Nu *vs.* Re

2.6. Modeling of ANFIS

As a method of learning, ANFIS converts inputs into outputs by means of densely linked neural networks and fuzzy logic. In order to build the model for this study, MATLAB was utilised. For each input, the default ANFIS function has utilised the dataset, the amount of membership functions (MFs), and kind of MFs to build the model structure. In order to create the FIS structure, the grid partitioning method was used. The MATLAB ANFIS uses combination of back-propagation gradient origin and least-squares methods to train network's parameters. The MF number stands for fuzzy rule numbers, which is supposed to be three, as shown in Figure 5.

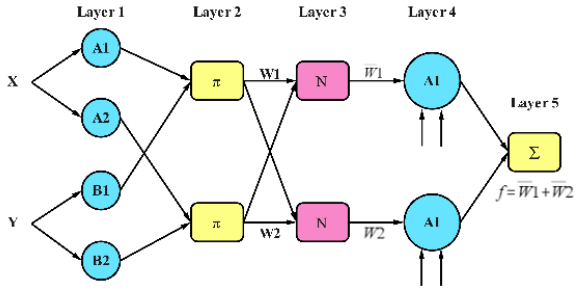

Figure 5. ANFIS architecture.

One common design for ANFIS is shown in Figure 5. Nodes that can be moved or repositioned are shown by the squares and circles, respectively, in this diagram. Here is a description of the layer's functionality along with the equations that support it:

Layer 1

The Fuzzification layer is the name of the initial layer. The aim of this layer is to get input values and find membership functions for inputs. This layer is responsible for transforming regular inputs into fuzzy ones. The membership function is fed fuzzy values, which is transformed from crisp values at top layer. Most of the time, the nodes in the first layer can be adjusted. A connection is made between the parameters and constant values of membership functions. According to [17], bell-type membership function was defined by equation (15).

$$mfij(x) = 11 + \{((x - ci)/ai)2\}bi \quad i,j = 1,2,3 \qquad (15)$$

Considering the membership function in this case is x. As it learns, the algorithm changes ai, bi, and ci. Different nodes may use different membership functions. The fuzziness in the structure is typically introduced by the layer.

Layer 2

Layer 2 is known as ruler layer The second layer takes the first layer's output as its input. The nodes in second layer cannot be changed. As shown in Eq. (16), At its first node, this layer multiplies the output of each input's initial membership function. The rule firing strengths are the outputs of these nodes. This causes the number of nodes and membership functions to equalise.

$$Wi=(mf\ 1j)(mf\ 2j)(mf\ 3j)\ \text{for}\ j=1,2,3 \quad (16)$$

Layer 3

In third and final layer, known as Normalization layer, the nodes standardise the firing skills acquired in the previous layer.

$$Win = Wi(W1 + W2 + W3) \quad (17)$$

Layer 4

Where fuzzy values are transformed into crisp values, this layer is called Defuzzification layer. The learning algorithm can modify the variables pi, qi, ri, and si at the adjustable nodes of the layer. The firing strength multiplies the nodes. The nodes' outputs are best understood in terms of:

$$Pi = Win\ (pix + qiy + si) \quad (18)$$

Layer 5

The output node gets its name from the fact that this layer's job is to aggregate all of the outputs from the levels below it. The following equation shows the system's final output [18]:

$$OP=\sum i=0npi \quad (19)$$

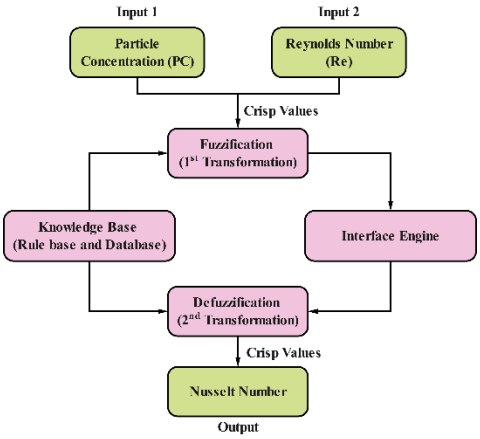

Figure 6. Flowchart of ANFIS working.

3. Results and Discussions

3.1. Input parameters

One output (Nu) and two inputs were used for ANFIS modelling. Nu was computed using the Pak-Cho correlation, and model was trained using Reynold's number ranging from 10,000 to 90,000 and PC from 0.5 to 4.5.

Table 1 shows the study's ANFIS parameters, which were automatically created using the fuzzy inference system (FIS).

Table 1. Parameters of ANFIS.

Parameters	Values
Nodes	203
Number of membership function for each input	9
Epoch	1,000
Number of fuzzy rules	81
Input membership function type	Triangular
Optimization method	Hybrid
FIS structure	Sugeno
Input membership function type	Constant

3.2. Membership functions

As can be observed in Figures 7 (a) and (b) , the MF's were automatically created by both inputs of ANFIS. The ANFIS modelling has been executed using triangular membership functions. The mathematical equation for the triangle membership functions used in this investigation was given by[19]:

$$\text{Triangular}(x,a,b,c)=\max(\min(x-a/b-a,1,c-x/c-b),0) \quad (20)$$

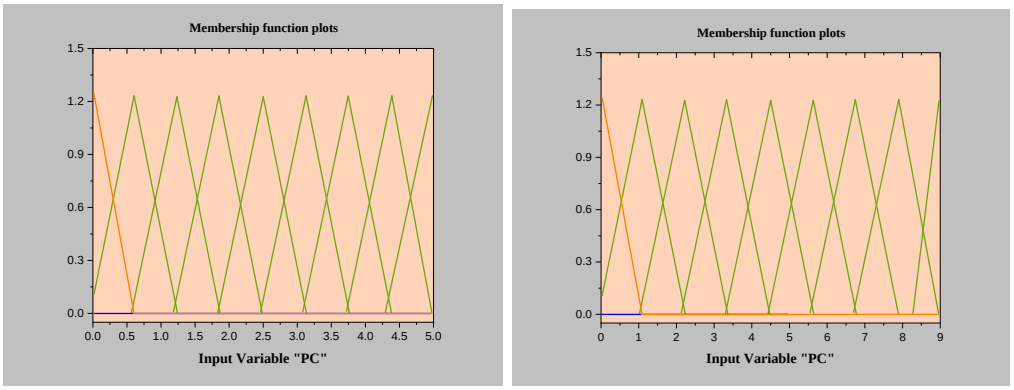

Figure 7 Membership functions (a)PC (b) Re.

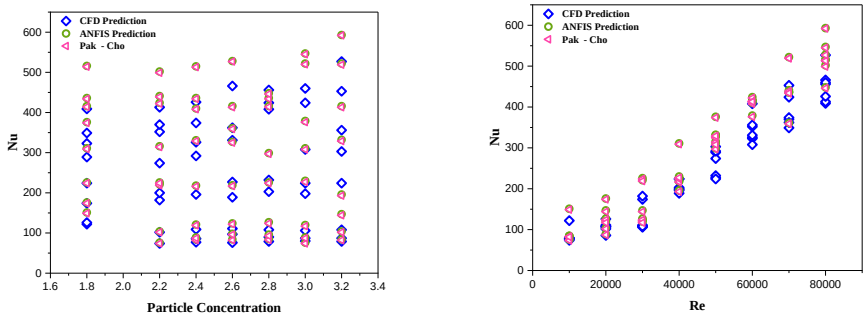

Figure 8. prediction of CFD vs. ANFIS.

The PC and Re values were used that were not in the training data at all to test ANFIS model. According to predictions of CFD Mixture model, the ANFIS model, and Pak and Cho correlation, the findings has been given as Nu with regard to Re. The Nu as a function of PC and Re changes are shown

in Figure 8 (a) and (b). There is some discrepancy in the CFD forecast, but for all relevant locations, the data predicted by ANFIS overlaps with Pak and Cho's experimental correlation prediction. To further understand the findings, the following figures show the relationship between Nu and Re for specific PCs.

The relationship between Nu and Re for PCs with a 2.2% PC and 3.2% PC is illustrated in Figures 9 (a) and (b). When comparing the two PCs, the CFD model has a far worse prediction error than the ANFIS model. While the Pak-Cho correlation and ANFIS forecast values are almost indistinguishable, it seems that the Mixture model underestimates the Nusselt number in all the cases. In reality, mean CFD errors calculated for these PC were 24.1% and 10.2%, respectively, while the ANFIS model only generated errors of 0.18% and 0.29%.

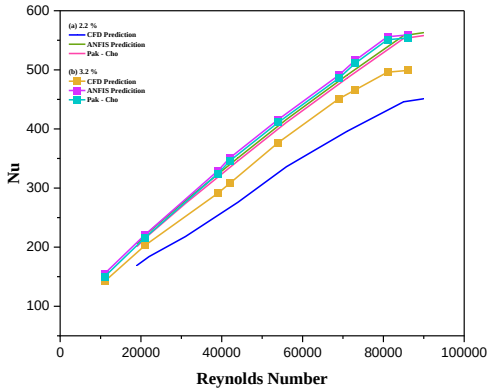

Figure 9. The particle concentration of Re vs Nu for (a) 2.2 % and (b) 3.2%

It appears that things take an intriguing turn for PCs of 3.5% and 3.9%. In Figures 10 (a) and (b), the Re range is shown with an average error of 2.1 % and a standard deviation of 1.2%, respectively, according to the Mixture model. In contrast, ANFIS forecasts Nu for identical scenarios with differences of 0.4% and 0.31%.

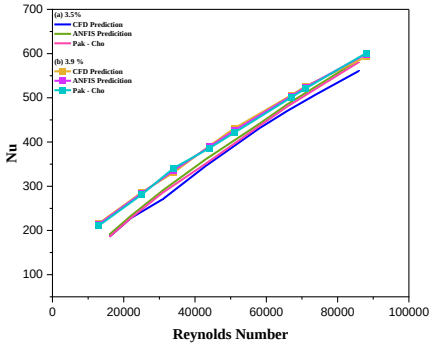

Figure 10. The particle concentration of Re vs Nu for (a) 3.5 % and (b) 3.9 %

Finally, when looking at PCs of 4.3% and 5%, as well as Reynolds number range shown in Figures 11 (a) and (b), ANFIS produces Nusselt number predictions with mean errors of 0.26% and 0.28%, respectively, while Mixture model overestimates Nu by 10.2% and 17.1% on average, respectively.

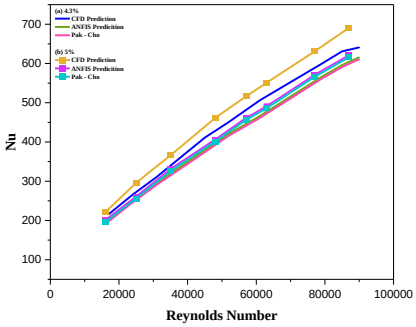

Figure 11. The particle concentration of Re vs Nu for (a) 4.3 % and (b) 5 %

The results show that ANFIS outperforms the CFD model in predicting Nu in every single situation. Actually, ANFIS predicts an average inaccuracy of 0.16 % to 0.38 % for every case. When it comes to estimating heat transfer enhancement, however, the Mixture model outperforms the other PCs with an average inaccuracy of about 2% when the PC is around 4%. Nu increases as Re and PC rise, as shown in the figures. The rising PC causes these effects because it alters the nanofluid's flow velocity and thermophysical characteristics. The authors' previous work [20]–[22] explains the reasons and repercussions of these actions.

Predictions made with the Mixture model are inaccurate for a number of reasons. Physical and geometrical modelling are only two of the many problems plaguing the CFD model. One of the main reasons why CFD results don't match experimental data is spatial discretization error. This is the difference between the exact solution to the partial differential equation and the numerical solution to the discretized equations. When solving differential equations, it is possible for higher-order terms to relax, which can lead to errors. Furthermore, computer round off errors and truncation error - the variations in partial differential and finite difference equations may contribute to inconsistencies between CFD and experimental data. It is the creation of the multiphase model that is to responsible for mistakes pattern shown by the Mixture model, in addition to the typical CFD flaws, as found in this work. First, the Mixture model overestimates the drag force at low mass loadings, which causes it to produce comparatively higher errors for both low and high PC. In reality, however, at low PC, the interphase interaction and, by extension, the drag force among primary and secondary phases was almost nonexistent. In experimental circumstances, increase in heat transmission is partially attributable to this lower drag force. Second, the Mixture model ignores the fact that nanoparticles' Brownian motion is significantly stronger in low PC due to decreased viscosity, density, and interparticle space, all of which contribute to an enhancement of heat transfer in real scenario. On flip side, heat transport is negatively impacted as Brownian motion decreases with increasing amounts of secondary mass loading.

However, ANFIS consistently produces highly accurate predictions of heat transfer enhancement. This is due to ANFIS, that develops the non-discrete domain in various dimensions, making it intelligent tool for local prediction of multiphase flows. When it comes to evaluating intricate engineering mechanisms, ANFIS can undertake complex simulations because to its intelligence inference engine. In addition, the approach is capable of identifying and fixing accuracy issues. Another method that uses a neuro-network to learn the process and uses the FIS for prediction is the ANFIS technique. Hence, a precise mathematical model is unnecessary. More so than the most nonlinear model, it works with imprecise inputs, handles nonlinearity, and displays disturbance insensitivity. In complicated, nonlinear, or undefined systems where there is strong practical knowledge, ANFIS performs better than other models.

4. Conclusion

An extensive variety of PC and Re values have been tested using the ANFIS and CFD Mixture models. The findings demonstrate that ANFIS consistently produces accurate results across all flow conditions, with a margin of error ranging from 0.16% to 0.38%. As a result, it can be utilised to forecast the improvement of heat transfer in water-Fe_2O_3 nanofluids regardless of the flow regime. However, for other nanofluid configurations, the CFD Mixture model deviates significantly, even though it approaches ANFIS 4% accuracy for PC. Therefore, while Mixture model and ANFIS can be employed equally for PC near 4%, ANFIS is clearly the superior choice for predicting heat transfer improvement for all other nanofluid configurations.

5. References

[1] L. S. Sundar, *et al.,* "ANFIS based effectiveness and number of transfer units predictions of MWCNT/water nanofluids flow in a double pipe U-bend heat exchanger," *Case Studies in Thermal Engineering*, 43, 2023.

[2] F. Selimefendigil and H. F. Öztop, "Magnetic field effects on the forced convection of CuO-water nanofluid flow in a channel with circular cylinders and thermal predictions using ANFIS," *Int J Mech Sci*, 146–147, 2018, pp. 9–24.

[3] F. Altarazi *et al.*, "Analysis and Implementation of Thermal Heat Exchanger Tube Performance with Helically Pierced Twisted Tape Inserts Using ANFIS Model," *Math Probl Eng*, 2021.

[4] T. Wen, *et al.,* "Experimental study on the thermal and flow characteristics of ZnO/water nanofluid in mini-channels integrated with GA-optimized ANN prediction and CFD simulation," *Int J Heat Mass Transf*, 178, 2021.

[5] H. Abazari Bahnemiri, *et al.*, "Numerical investigation and artificial brain structure-based modeling to predict the heat transfer of hybrid Ag/Au nanofluid in a helical tube heat exchanger," *Advances in Mechanical Engineering*, 15, 2023.

[6] M. E. Polat and S. Cadirci, "Artificial neural network model and multi-objective optimization of microchannel heat sinks with diamond-shaped pin fins," *Int J Heat Mass Transf*, 194, 2022.

[7] P. Dey, *et al.,* "Development of GEP and ANN model to predict the unsteady forced convection over a cylinder," *Neural Comput Appl*, 27, 2016, 8, pp. 2537–2549.

[8] A. Tikadar and S. Kumar, "Machine learning approach to predict heat transfer and fluid flow characteristics of integrated pin fin-metal foam heat sink," *Numerical Heat Transfer, Part B: Fundamentals*, 2023.

[9] A. P. Koroleva, *et al.,* "Application of machine learning methods for investigating the heat transfer enhancement performance in a circular tube with artificial roughness," in *Journal of Physics: Conference Series*, 2020.

[10] K. L. Liaw, *et al.,* "Enhanced turbulent convective heat transfer in helical twisted Multilobe tubes," *Int J Heat Mass Transf*, 202, 2023.

[11] V. Leela, *et al.,* "Computational analysis of ohmic and viscous dissipation effects on MHD mixed convection flow in a vertical channel with linearly varying wall temperatures," *Proceedings of the Institution of Mechanical Engineers, Part E: Journal of Process Mechanical Engineering*, 2022.

[12] A. Tikadar and S. Kumar, "Investigation of thermal-hydraulic performance of metal-foam heat sink using machine learning approach," *Int J Heat Mass Transf*, 199, 2022.

[13] N. Hajialigol and R. Daghigh, "The evaluation of the first and second laws of thermodynamics for the pulsating MHD nanofluid flow using CFD and machine learning approach," *J Taiwan Inst Chem Eng*, 148, 2023.

[14] M. Darvish Damavandi, *et al.*, "Pareto optimal design of swirl cooling chambers with tangential injection using CFD, GMDH-type of ANN and NSGA-II algorithm," *International Journal of Thermal Sciences*, 122, 2017, pp. 102–114.

[15] A. P. Koroleva, *et al.*, "Investigation on heat transfer enhancement in a circular pipe with artificial roughness," in *Journal of Physics: Conference Series*, 2020.

[16] E. Ayli and E. Kocak, "Prediction of the heat transfer performance of twisted tape inserts by using artificial neural networks," *Journal of Mechanical Science and Technology*, 36, 2022, 9, pp. 4849–4858.

[17] M. M. Tafarroj, *et al.*, "Multi-purpose prediction of the various edge cut twisted tape insert characteristics: multilayer perceptron network modeling," *J Therm Anal Calorim*, 145, 2021, 4, pp. 2005–2020.

[18] R. Girimurugan *et al.*, "Application of Deep Learning to the Prediction of Solar Irradiance through Missing Data," *International Journal of Photoenergy*, 2023.

[19] W. Alghamdi, *et al.*, "Turbulence Modeling Through Deep Learning: An In-Depth Study of Wasserstein GANs," 2023.

[20] E. Aslan, *et al.*, "LBM curved boundary treatments for pulsatile flow on convective heat transfer and friction factor in corrugated channels," *Proc Inst Mech Eng C J Mech Eng Sci*, 2023.

[21] P. Dey and A. Das, "Numerical analysis and prediction of unsteady forced convection over a sharp and rounded edged square cylinder," *Journal of Applied Fluid Mechanics*, 9 2016, 3, pp. 1189–1199.

[22] S. Salimi, *et al.*, "Heat transfer enhancement of serpentine channels with twisted tape insert by computational fluid dynamics and artificial intelligence," *Canadian Journal of Chemical Engineering*, 2023.

Received: 12-04-2023

Revised: 19-10-2023

Accepted: 15-11-2023